


RESEARCH

Open Access



IL-1RA promotes oral squamous cell carcinoma malignancy through mitochondrial metabolism-mediated EGFR/JNK/SOX2 pathway

Shyng-Shiou F. Yuan^{1,2,3,4,5,6}, Yun-Ming Wang^{6,7}, Leong-Perng Chan^{8,9,10}, Amos C. Hung¹, Hieu D. H. Nguyen⁷, Yuk-Kwan Chen^{7,11}, Stephen Chu-Sung Hu^{12,13}, Steven Lo^{14,15} and Yen-Yun Wang^{2,5,7*} 

Abstract

Background Interleukin-1 receptor antagonist (IL-1RA), a member of the IL-1 family, has diverse roles in cancer development. However, the role of IL-1RA in oral squamous cell carcinoma (OSCC), in particular the underlying mechanisms, remains to be elucidated.

Methods Tumor tissues from OSCC patients were assessed for protein expression by immunohistochemistry. Patient survival was evaluated by Kaplan–Meier curve analysis. Impact of differential IL-1RA expression on cultured OSCC cell lines was assessed in vitro by clonogenic survival, tumorsphere formation, soft agar colony formation, and transwell cell migration and invasion assays. Oxygen consumption rate was measured by Seahorse analyzer or multi-mode plate reader. PCR array was applied to screen human cancer stem cell-related genes, proteome array for phosphorylation status of kinases, and Western blot for protein expression in cultured cells. In vivo tumor growth was investigated by orthotopic xenograft in mice, and protein expression in xenograft tumors assessed by immunohistochemistry.

Results Clinical analysis revealed that elevated IL-1RA expression in OSCC tumor tissues was associated with increased tumor size and cancer stage, and reduced survival in the patient group receiving adjuvant radiotherapy compared to the patient group without adjuvant radiotherapy. In vitro data supported these observations, showing that overexpression of IL-1RA increased OSCC cell growth, migration/invasion abilities, and resistance to ionizing radiation, whereas knockdown of IL-1RA had largely the opposite effects. Additionally, we identified that EGFR/JNK activation and SOX2 expression were modulated by differential IL-1RA expression downstream of mitochondrial metabolism, with application of mitochondrial complex inhibitors suppressing these pathways. Furthermore, in vivo data revealed that treatment with cisplatin or metformin—a mitochondrial complex inhibitor and conventional therapy for type 2 diabetes—reduced IL-1RA-associated xenograft tumor growth as well as EGFR/JNK activation and SOX2 expression. This inhibitory effect was further augmented by combination treatment with cisplatin and metformin.

Conclusions The current study suggests that IL-1RA promoted OSCC malignancy through mitochondrial metabolism-mediated EGFR/JNK activation and SOX2 expression. Inhibition of this mitochondrial metabolic pathway may present a potential therapeutic strategy in OSCC.

Keywords IL-1RA, Mitochondrial metabolism, EGFR, JNK, SOX2, Cancer stemness, Tumor growth, Metastasis, OSCC

*Correspondence:

Yen-Yun Wang

wyy@kmu.edu.tw

Full list of author information is available at the end of the article



© The Author(s) 2023. **Open Access** This article is licensed under a Creative Commons Attribution 4.0 International License, which permits use, sharing, adaptation, distribution and reproduction in any medium or format, as long as you give appropriate credit to the original author(s) and the source, provide a link to the Creative Commons licence, and indicate if changes were made. The images or other third party material in this article are included in the article's Creative Commons licence, unless indicated otherwise in a credit line to the material. If material is not included in the article's Creative Commons licence and your intended use is not permitted by statutory regulation or exceeds the permitted use, you will need to obtain permission directly from the copyright holder. To view a copy of this licence, visit <http://creativecommons.org/licenses/by/4.0/>. The Creative Commons Public Domain Dedication waiver (<http://creativecommons.org/publicdomain/zero/1.0/>) applies to the data made available in this article, unless otherwise stated in a credit line to the data.

Background

Oral cancer is one of the most prevalent cancers and causes of cancer-related deaths worldwide, and oral squamous cell carcinoma (OSCC) is the most frequently diagnosed form of oral cancer [1–3]. Various risk factors promote oral cancer development, including tobacco use, alcohol consumption, and betel quid [4]. However, the management of oral cancer remains a challenge owing to its tendency for frequent relapse, metastasis, and treatment resistance [4–6]. An important potential mechanism underlying some of these oncological challenges is the property of cancer stemness, which is associated with the enhanced self-proliferation and metastatic ability of cancer cells. Recent research has suggested that altered mitochondrial metabolism underpins some of these malignant cell characteristics [7–10].

The interleukin-1 (IL-1) family includes both pro- or anti-inflammatory proteins, with pro-inflammatory IL-1 β being the best characterized one [11]. On the other hand, interleukin-1 receptor antagonist (IL-1Ra) is a natural anti-inflammatory antagonist of the interleukin-1 family of pro-inflammatory cytokines [12]. IL-1RA, the gene product of *IL1RN* which shares approximately 30% protein sequence homology with interleukin-1 (IL-1), competes with IL-1 for binding to the IL-1 receptor [13, 14]. As a member of the IL-1 family with multifaceted functions, IL-1RA plays diverse roles in a number of pathological conditions, including cancer. For example, lower levels of IL-1RA were found in several cancer types, such as leukemia, colorectal cancer, and prostate cancer [15–17], and it was negatively associated with the development of premalignant oral dysplasia [18]. However, other reports indicate higher levels of IL-1RA in cervical and gastric cancers [19, 20], suggesting that IL-1RA may function in a cancer type-specific manner. However, its clinical role and biological function in oral cancer development remain unclear. Accumulating evidence has linked the development of oral cancer with IL-1-mediated chronic inflammation [21]. It is intriguing to investigate whether IL-1RA, an anti-inflammatory antagonist of IL-1, also plays a role in oral carcinogenesis.

In this study, we evaluated the potential of IL-1RA as a clinical marker for OSCC progression and patient outcomes. In addition, the cellular mechanisms of IL-1RA in OSCC malignancy were explored both in vitro and in vivo, providing insights into the development of novel therapeutic strategies for OSCC that target vulnerabilities in the IL-1RA-associated mitochondrial metabolic pathway.

Methods

Patient samples

Oral tumor tissues were obtained from patients diagnosed with OSCC at the Department of Oral and Maxillofacial Surgery, Kaohsiung Medical University Hospital, Kaohsiung, Taiwan, and confirmed using clinical and histological data from the Cancer Registry. Overall survival was defined as the interval between the date of diagnosis and date of death. This study was approved by the Institutional Review Board of Kaohsiung Medical University Hospital (approval no. KMUH-IRB-20130300 and KMUHIRB-F(1)-20220016). Patient informed consent was waived by the Institutional Review Board due to the retrospective nature of the study.

Cell culture

Human oral squamous cell carcinoma cell lines HSC-3, Ca9-22, and OECM-1 were obtained from the Bioresource Collection and Research Center, Hsinchu, Taiwan (<https://www.bcrc.firdi.org.tw>). HSC-3 and Ca9-22 cells were cultured in DMEM/F12 medium (Thermo Fisher Scientific, Waltham, MA, USA), and OECM-1 cells were cultured in RPMI 1640 medium (Thermo Fisher Scientific, Waltham, MA, USA). All cell culture media were supplemented with 10% fetal bovine serum (FBS; Biological Industries, Beit Haemek, Israel) and 1% penicillin–streptomycin–amphotericin B (Thermo Fisher Scientific, Waltham, MA, USA). Cells were maintained at 37 °C in a humidified incubator with 5% CO₂ incubator.

Gene knockdown and overexpression

Knockdown of IL-1RA was conducted by lentiviral infection using a pLKO.1-puro vector carrying shRNA sequences (shIL-1RA#1, 5'-GCCTTCAGAAATCTGGGATGTT-3'; shIL-1RA#2, 5'-CGAGAACAGAAAGCAGGACAA-3'; shIL-1RA#3, 5'-GCAAGGACCAAATGTCAATTT-3'; shIL-1RA#4, 5'-CGTCATGGTCACCAAATTCTA-3') that target consensus regions of human *IL1RN* (Accession: NM_000577), which were obtained from the National RNAi Core Facility, Academia Sinica, Taipei, Taiwan. Another pLKO.1-puro vector carrying shRNA sequences targeting firefly luciferase (shLuc, 5'-GCGGTTGCCAAGAGGTTCCAT-3') was used as a control (National RNAi Core Facility, Academia Sinica, Taipei, Taiwan). For gene overexpression of IL-1RA, pre-packaged lentiviral particles carrying pReceiver-Lv105 vector expressing full-length human *IL1RN* (IL-1RA-OE; Accession: NM_173841.2), or empty pReceiver-Lv105 vector (EV) as a control, were purchased from GeneCopoeia (Rockville, MD, USA). The infection was performed by adding lentiviral particles to the corresponding cells in the cell culture medium containing 8 μ g/mL polybrene

(Sigma-Aldrich, St. Louis, MO, USA). After infection for 48 h, 2 µg/mL puromycin was added for selection, and the surviving cells were maintained in 2 µg/mL puromycin until further experiments.

Clonogenic survival assay

OSCC cells were seeded in 6-well plates (1×10^3 cells/well; Corning, Tewksbury, MA, USA) and cultured for 14 days prior to staining with 0.5% crystal violet (Sigma-Aldrich, St. Louis, MO, USA) for 15 min at room temperature. For ionizing radiation treatment, cells were irradiated at a dose of 5 Gy using a 6-MV linear accelerator (Elekta, Stockholm, Sweden) at the Department of Radiation Oncology, Kaohsiung Medical University Hospital, Kaohsiung, Taiwan. Images were captured using a light microscope (Nikon, Tokyo, Japan) and analyzed using ImageJ software (<https://imagej.nih.gov/ij/>).

Tumorsphere formation assay

OSCC cells were seeded in ultra-low attachment 96-well plates (5×10^2 cells/well; Corning, Tewksbury, MA, USA) in serum-free cell culture medium supplemented with 20 ng/ml epidermal growth factor (EGF; PeproTech, Rehovot, Israel), 20 ng/ml fibroblast growth factor-basic (FGF-basic; PeproTech), 10 µg/mL insulin (Sigma-Aldrich, St. Louis, MO, USA), and 1X B27 (Thermo Fisher Scientific, Waltham, MA, USA). After 14 days of cell culture, images of tumorspheres larger than 50 µm in diameter were captured using a light microscope (Nikon, Tokyo, Japan) and analyzed with ImageJ (<https://imagej.nih.gov/ij/>).

Soft agar colony formation assay

OSCC cells were suspended in cell culture medium mixed with 0.4% low-melting agarose (Sigma-Aldrich, St. Louis, MO, USA) and then seeded in 6-cm dishes (1×10^4 cells/dish; Corning, Tewksbury, MA, USA) pre-coated with a layer of 0.5% low-melting agarose (Sigma-Aldrich, St. Louis, MO, USA). After 14 days of cell culture, colonies larger than 100 µm in diameter were stained with 0.5% crystal violet for 15 min at room temperature, and images were captured using a stereo microscope (Olympus, Tokyo, Japan) and analyzed with ImageJ (<https://imagej.nih.gov/ij/>).

XTT cell viability assay

OSCC cells were seeded in 96-well plates (1×10^4 cells/well; Corning, Tewksbury, MA, USA) for 24 h, prior to the addition of XTT reagent from Cell Proliferation Kit II (Sigma-Aldrich, St. Louis, MO, USA) for 2 h at 37 °C, followed by measurement of the optical density (OD) at 470 nm by subtracting the background at 660 nm.

Transwell cell migration and invasion assays

OSCC cells were re-suspended in serum-free cell culture medium and plated onto inserts (2×10^4 cells/insert; 8 µm pores) in 24-well transwell plates (Corning, Tewksbury, MA, USA). The inserts were pre-coated with or without Matrigel (Corning, Tewksbury, MA, USA) for cell invasion and migration assays, respectively, and normal cell culture medium was added to the bottom wells. After 24 h, cells that remained on the upper side of the inserts were removed using cotton swabs, and cells that appeared on the lower side of the inserts were fixed with 4% formaldehyde (Sigma-Aldrich, St. Louis, MO, USA) for 15 min and stained with 0.05% crystal violet (Sigma-Aldrich, St. Louis, MO, USA) for 30 min at room temperature. Images were captured using a light microscope (Nikon, Tokyo, Japan) and analyzed using ImageJ software (<https://imagej.nih.gov/ij/>).

Measurement of oxygen consumption rate (OCR) and extracellular acidification rate (ECAR)

The basal OCR and ECAR of OSCC cells were measured using the Extracellular Oxygen Consumption Assay and Glycolysis Assay kits (Abcam, Waltham, MA, USA), respectively, according to the manufacturer's instructions. The fluorescent signal was measured using a CLARIOstar Plus multi-mode plate reader (BMG Labtech, Ortenberg, Germany) at 1.5 min intervals with excitation/emission wavelengths of 360/650 nm for OCR and 380/615 nm for ECAR. To measure multiple statuses of OCR in mitochondria, an Agilent Seahorse XFe24 Analyzer (Agilent Technologies, Santa Clara, CA, USA) was used in accordance with the procedures from the manufacturer and our previous report [22]. The mitochondrial modulators were obtained from Seahorse XF Cell Mito Stress Test Kit (Agilent Technologies, Santa Clara, CA, USA) and injected sequentially for specific measurements as follows: first, 1 µM oligomycin was injected to measure ATP production; second, 0.5 µM carbonyl cyanide 4-(trifluoromethoxy)phenylhydrazone (FCCP) was injected to measure maximal respiration; finally, 0.5 µM rotenone and 0.5 µM antimycin A were injected to measure spare respiratory capacity [23].

Measurement of reactive oxygen species (ROS) formation

OSCC cells were seeded in 6-well plates (3×10^5 cells/well) overnight, followed by labeling with 10 µM 2',7'-dichlorofluorescein diacetate (DCFDA; Sigma-Aldrich, St. Louis, MO, USA) for 20 min at room temperature. The cells were then analyzed using a Cytomics FC 500 Flow Cytometer (Beckman Coulter, Indianapolis, IN,

USA) in accordance with the manufacturer's instructions and our previous report [22].

Polymerase chain reaction (PCR) array

Total RNA extracted from OSCC cells was reverse transcribed and analyzed by real-time PCR using the Human Stem Cell Signaling RT² Profiler PCR Array (Qiagen, Redwood City, CA, USA) according to the manufacturer's instructions and our previous report [24].

Proteome array

Total protein extracted from OSCC cells was analyzed using the Human Phospho Kinase Array (R&D Systems, Minneapolis, MN, USA), according to the manufacturer's instructions and our previous reports [25, 26].

Western blot

Total protein extracted from OSCC cells was separated by sodium dodecyl sulfate–polyacrylamide gel electrophoresis (SDS-PAGE), followed by transferred onto nitrocellulose membranes (Merck, Darmstadt, Germany). The membranes were blocked with 2% skimmed milk (Anchor, Auckland, New Zealand) and incubated with primary antibodies overnight, followed by further incubation with species-matched horseradish peroxidase-conjugated secondary antibodies (Thermo Fisher Scientific, Waltham, MA, USA) for 1 h at room temperature. Immunoreactive protein bands were detected by incubation with Immobilon Western chemiluminescent reagents (Merck, Darmstadt, Germany), and the signals were captured by ChemiDoc XRS+ (Bio-Rad, Hercules, CA, USA) and analyzed with Image Lab (Bio-Rad, Hercules, CA, USA). The following primary antibodies were used for Western blot: Goat anti-human IL-1RA (R&D Systems, Minneapolis, MN, USA), rabbit anti-human SOX2 (GeneTex, Hsinchu, Taiwan), rabbit anti-human EGF (GeneTex, Hsinchu, Taiwan), rabbit anti-human THY1 (Abcam, Waltham, MA, USA), rabbit anti-human c-KIT (Cell Signaling Technology, Danvers, MA, USA), rabbit anti-human p21 (GeneTex, Hsinchu, Taiwan), rabbit anti-human phospho-EGFR at Tyr1086 (GeneTex, Hsinchu, Taiwan), rabbit anti-human EGFR (GeneTex, Hsinchu, Taiwan), rabbit anti-human phospho-JNK1/2/3 at Thr183 (Abcam, Waltham, MA, USA),

rabbit anti-human JNK1/2/3 (Abcam, Waltham, MA, USA), rabbit anti-human GAPDH (GeneTex, Hsinchu, Taiwan), and mouse anti-human β -actin (Sigma-Aldrich, St. Louis, MO, USA).

Immunohistochemistry (IHC)

Formalin-fixed and paraffin-embedded normal and tumor tissue sections were immunostained using a Bond-Max automated IHC stainer (Leica Microsystems, Wetzlar, Germany) in accordance with the manufacturer's instructions and our previous reports [24, 27]. The following primary antibodies were used for IHC: goat anti-human IL-1RA (R&D Systems, Minneapolis, MN, USA), rabbit anti-human SOX2 (GeneTex, Hsinchu, Taiwan), rabbit anti-human Ki67 (GeneTex, Hsinchu, Taiwan), rabbit anti-human phospho-EGFR at Tyr1086 (GeneTex, Hsinchu, Taiwan), and rabbit anti-human phospho-JNK1/2/3 at Thr183/Thr183/Thr221 (Abcam, Waltham, MA, USA). IHC images were captured using an Eclipse E600 microscope (Nikon, Tokyo, Japan), and total immunostaining scores for each tissue section were determined as the product of the percentage of positively stained cells (0, 0–4%; 1, 5–24%; 2, 25–49%; 3, 50–74%; 4, 75–100%) multiplied by the intensity of staining (0, negative; 1, weak; 2, moderate; 3, strong). To further analyze the association between IL-1RA expression and patient survival, the expression level of IL-1RA by IHC scoring was categorized into low versus high expression with cut-off values according to ROC curves [24, 27].

Animal study

Experiments involving animals were approved by and in accordance with the guidelines and regulations of the Institutional Animal Care and Use Committee of Kaohsiung Medical University, Kaohsiung, Taiwan (Approval no. 108127). Three-week-old male NOD.CB17-*Prkdc*^{scid}/JNarl mice were obtained from the National Laboratory Animal Center of Taiwan (<https://www.nlac.narl.org.tw>). For orthotopic xenografts, OECM-1 cells expressing luciferase (OECM-1-luc; 5×10^5 cells per mouse) resuspended in 100 μ L of phosphate-buffered saline were injected into mice through the intrabuccal route. At 1 week post-xenograft, the mice were randomly assigned to eight groups (five mice per group), including

(See figure on next page.)

Fig. 1 Association of IL-1RA expression with OSCC progression and patient outcomes. **A** Protein expression of IL-1RA in oral tumor tissues from OSCC patients (OSCC) and normal oral tissues from normal epithelial regions of fibroma patients (Normal) was analyzed by immunohistochemistry (IHC). The negative control for IL-1RA staining was performed in parallel with omission of primary antibodies. **B–C** Protein expression of IL-1RA in OSCC tumor tissues was analyzed by IHC for the comparison of primary tumor size (T1 versus T2–T4) in **(B)**, and cancer stage (Stage I versus Stage II–IV) in **(C)**. The scoring of IHC was described in the Methods section. Data were presented as mean \pm SD with the indicated sample size in parentheses. *, $p < 0.05$; **, $p < 0.01$. **D** Overall survival probability was analyzed by Kaplan–Meier survival curves for patients with adjuvant radiotherapy (+) and patients without adjuvant radiotherapy (–) according to the expression level of IL-1RA in OSCC tumor tissues (low versus high) as described in the Methods section. The sample size in each group was indicated in parentheses

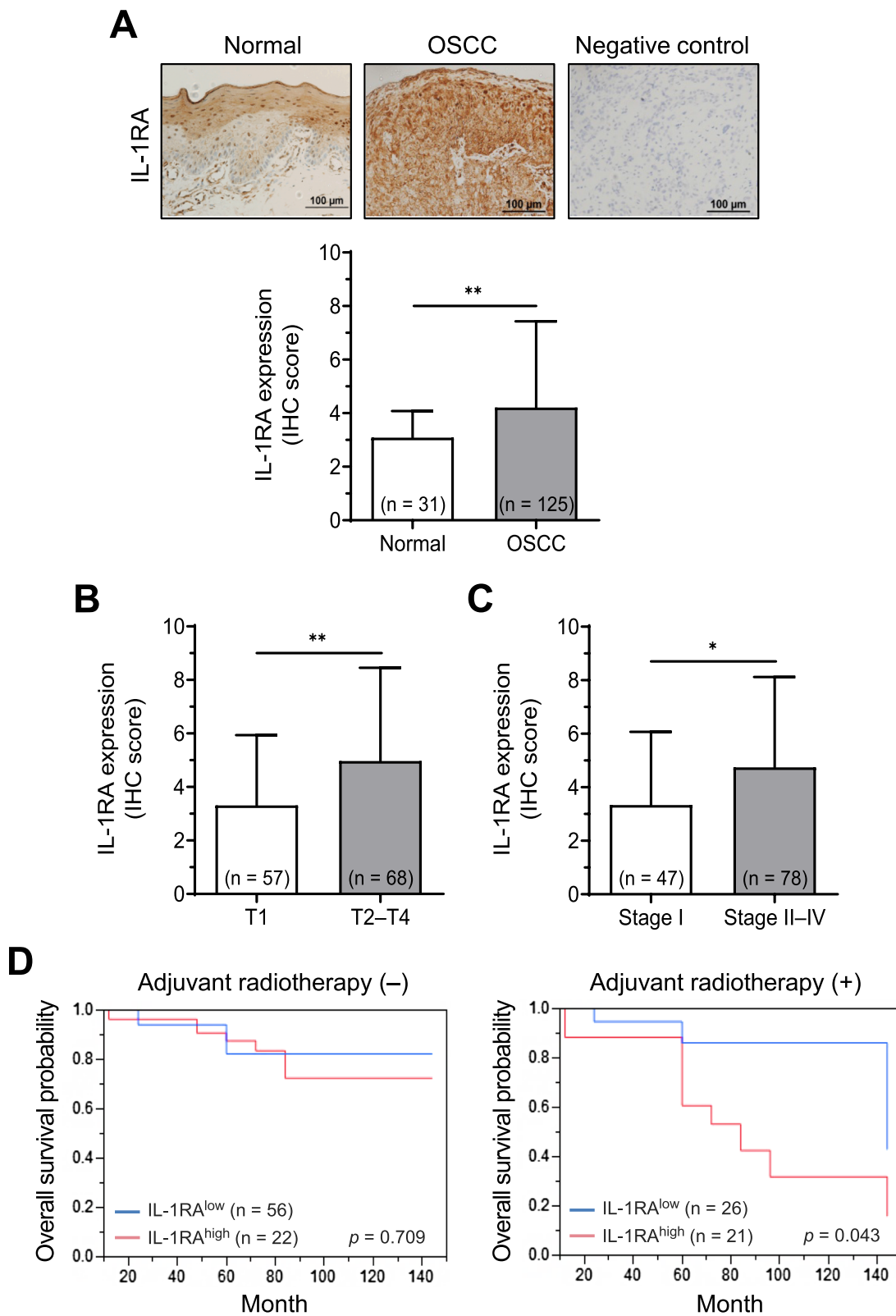


Fig. 1 (See legend on previous page.)

empty vector (EV) versus IL-1RA-OE from each of the untreated, metformin-treated, cisplatin-treated, and metformin combined with cisplatin-treated groups. The untreated groups were intraperitoneally injected with normal saline thrice per week. The metformin-treated group (200 mg/kg) was injected intraperitoneally three times per week. The cisplatin-treated group (2 mg/kg) was injected intraperitoneally once per week. In the metformin combined with cisplatin-treated groups, metformin (200 mg/kg) was administered three times per week and cisplatin (2 mg/kg) was administered once per week. All mice were monitored weekly using an IVIS Spectrum in vivo imaging system (PerkinElmer, Santa Clara, CA, USA), according to the manufacturer's instructions and our previous report [24]. After treatment for 5 weeks, the mice were sacrificed, and orthotopic xenograft tumors were collected for tumor weight and volume measurements, followed by immunohistochemical analysis.

Statistical analysis

Statistical analyses were performed using JMP version 10.0.1 for Windows (SAS Institute, Cary, NC, USA). The log-rank test was used to compare patient survival using Kaplan–Meier curve analysis. The Student's *t*-test was used to compare the two groups. One-way analysis of variance (ANOVA) with post-hoc Tukey's test was used for multiple group comparisons. Pearson correlation (*r*) was used to evaluate the correlation between the two protein expression levels by IHC. The data are presented as the mean ± SD from three independent experiments where applicable or as otherwise specified in individual figures. *P* values less than 0.05 were considered statistically significant.

Results

Clinical association of IL-1RA expression with OSCC progression and patient outcomes

To evaluate the association between IL-1RA expression and OSCC progression, immunohistochemical analysis was performed on OSCC tumor tissues and normal oral mucosal tissues adjacent to the oral fibroma tissues for comparison. The results indicated an elevated level of IL-1RA expression in OSCC tumor tissues compared to that in the normal oral mucosa ($p=0.001$; Fig. 1A). Further analysis of the clinicopathological characteristics

revealed that elevated IL-1RA expression in OSCC tumor tissues was associated with tumor size ($p=0.003$; Fig. 1B) and cancer stage ($p=0.012$; Fig. 1C). Moreover, there was an association between the expression of IL-1RA and the overall survival of patients with OSCC in response to treatment, in which high IL-1RA expression was associated with poorer overall survival probability in patients receiving adjuvant radiotherapy, but this association was not observed in patients who did not receive adjuvant radiotherapy ($p=0.043$ and 0.709 , respectively; Fig. 1D). These clinical data suggest that elevated IL-1RA expression is associated with adverse OSCC progression and poor treatment outcomes. Therefore, we performed gene knockdown and overexpression of IL-1RA in OSCC cells to investigate the impact of differential IL-1RA expression on cancer cell malignancy.

IL-1RA promoted in vitro cancer cell growth and migration/invasion abilities via the mitochondrial metabolic pathway

Different levels of endogenous IL-1RA expression were detected in four human OSCC cell lines, including HSC-3, SAS, Ca9-22, and OECM-1, with HSC-3 and Ca9-22 cells showing higher IL-1RA expression than SAS and OECM-1 cells (Additional file 1: Figure S1A). A screen for knockdown clones of IL-1RA revealed better efficacy of shIL-1RA#1 and #2 (Additional file 1: Figure S1B). Therefore, in subsequent studies, HSC-3 and Ca9-22 cells were selected for gene knockdown of IL-1RA by shIL-1RA#1 and #2 and OECM-1 cells for gene overexpression of full-length IL-1RA (Additional file 1: Figure S1C).

Colony forming assay and tumorsphere formation assay have been used for the determination of cancer cell stemness [28, 29]. Using a clonogenic survival assay, we observed that knockdown of IL-1RA in HSC-3 and Ca9-22 cells reduced cancer cell growth (Fig. 2A), whereas overexpression of IL-1RA in OECM-1 cells increased cancer cell growth (Fig. 2B). Furthermore, knockdown of IL-1RA in HSC-3 cells reduced tumorsphere formation (Fig. 2C), whereas overexpression of IL-1RA in OECM-1 cells increased tumorsphere formation (Fig. 2D). In addition, overexpression of IL-1RA in OECM-1 cells enhanced colony formation on soft agar (Fig. 2E). Analysis of the cell cycle distribution revealed that knockdown of IL-1RA in HSC-3 cells led to increased G0/G1 phase and decreased G2/M phase (Additional file 1: Figure S2A), whereas overexpression of IL-1RA in

(See figure on next page.)

Fig. 2 Effect of IL-1RA expression on in vitro cell growth of OSCC cells. **A–F** Following knockdown of IL-1RA expression in HSC-3 and Ca9-22 cells and overexpression of IL-1RA in OECM-1 cells, assessments were performed for clonogenic survival (**A, B**), tumorsphere formation (**C, D**), and colony formation in soft agar (**E**). In (**F**), clonogenic survival was assessed in OECM-1 cells with overexpression of IL-1RA and control cells in the presence or absence of ionizing radiation treatment. Data were presented as mean ± SD from three independent experiments. *, $p < 0.05$; **, $p < 0.01$; ***, $p < 0.001$. shLuc, knockdown of firefly luciferase; shIL-1RA, knockdown of IL-1RA; EV, empty vector; IL-1RA-OE, overexpression of IL-1RA

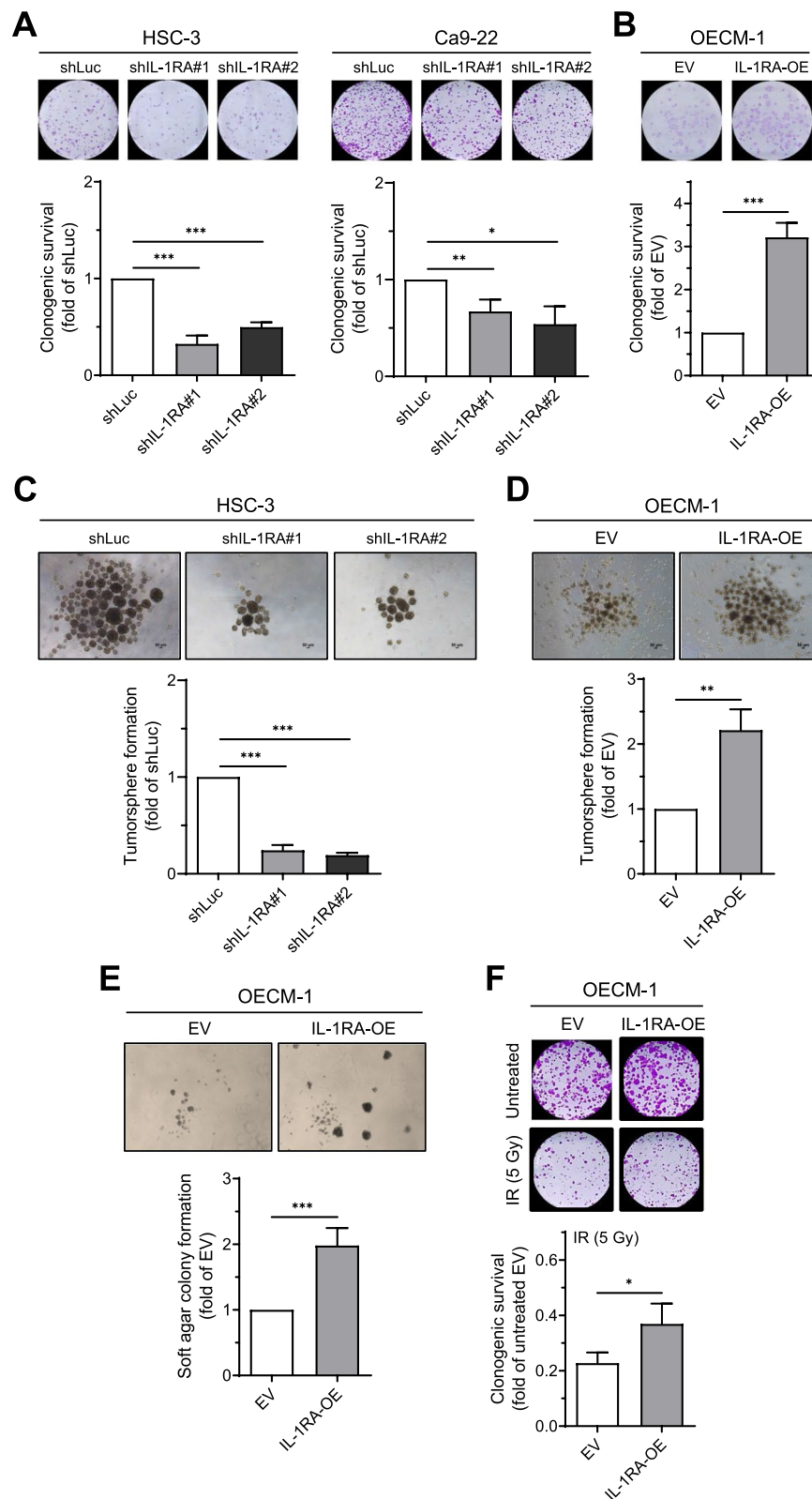


Fig. 2 (See legend on previous page.)

OECM-1 cells had the opposite effect on cell cycle distribution (Additional file 1: Figure S2B). Concordantly, the expression of p21 was increased in HSC-3 cells with knockdown IL-1RA but decreased in OECM-1 cells overexpressing IL-1RA (Additional file 1: Figure S2C and D). To examine the effect of IL-1RA expression on cancer cell growth under the influence of ionizing radiation (IR), OECM-1 cells were treated with IR followed by a clonogenic survival assay. We found that while ionizing irradiation caused a significant reduction in cell growth in both IL-1RA overexpression and control EV groups, the IL-1RA overexpression group had more surviving cells after IR treatment than the EV controls (Fig. 2F). These data indicate that alteration of IL-1RA expression affects cancer cell growth in OSCC cells, including clonogenic survival and colony formation in soft agar, and tumor-sphere formation, which represent the properties of cancer stemness-associated growth [30–32].

Mitochondrial metabolism has been implicated in oncogenesis, such as the acquisition of cancer stemness properties, metastatic ability, and radioresistance [7, 9, 33]. In this study, we demonstrated that IL-1RA positively correlated with cancer cell stemness (Fig. 2). Therefore, we further examined the role of mitochondrial metabolism in IL-1RA-associated oral cancer cell malignancy. As shown in Fig. 3A, overexpression of IL-1RA in OECM-1 cells increased the oxygen consumption rate (OCR), an indicator of mitochondrial oxidative phosphorylation [34, 35], as indicated by the upregulated basal OCR, ATP production, and maximal respiration using the Seahorse Analyzer. In concordance with this result, altered basal OCR was observed in HSC-3 cells with knockdown of IL-1RA and in OECM-1 cells overexpressing IL-1RA using a different apparatus (Fig. 3B and C). In contrast, Additional file 1: Figure S3A and B show that the effect of differential IL-1RA expression on the extracellular acidification rate (ECAR; an indicator of glycolytic level [34, 35] was the opposite compared to the results of OCR in Fig. 3B and C. Levels of reactive oxygen species (ROS) were increased by overexpression of IL-1RA in OECM-1 cells and were reduced in the presence of the mitochondrial complex inhibitor rotenone (Fig. 3D), metformin, and phenformin (Fig. 3E) [36, 37]. Furthermore, application of mitochondrial complex inhibitors to

OECM-1 cells overexpressing IL-1RA effectively reduced IL-1RA-promoted tumorsphere formation (Fig. 4A and B). IL-1RA-promoted cell migration (Fig. 4C, D, and Additional file 1: Figure S4A) and invasion (Fig. 4E) in OECM-1 cells were also reduced by mitochondrial complex inhibitors under circumstances where these inhibitors did not affect the viability of OECM-1 cells within the same time window of treatment (Additional file 1: Figure S4B–D). Altogether, these data suggest that IL-1RA-promoted OSCC malignant behaviors, such as tumorspheric growth and cell migration/invasion abilities, are mediated through the mitochondrial metabolic pathway.

Involvement of mitochondrial metabolism in IL-1RA-associated SOX2 expression

To investigate the potential involvement of cancer stemness-related genes in IL-1RA-promoted OSCC malignancy, a screening approach using a PCR array was applied, which showed that four stemness markers, including *SOX2*, *THY1*, *EGF*, and *KIT*, were most downregulated in HSC-3 cells with IL-1RA knockdown (Fig. 5A and Additional file 1: Figure S5). The protein expression levels of these four candidates were further examined by western blotting, which showed that *SOX2* was consistently downregulated in HSC-3 and Ca9-22 cells with IL-1RA knockdown (Fig. 5B) and upregulated in OECM-1 cells overexpressing IL-1RA (Fig. 5C). Moreover, IL-1RA-promoted *SOX2* expression in OECM-1 cells was reduced in the presence of mitochondrial complex inhibitors (Fig. 5D), suggesting that the effect of IL-1RA on *SOX2* expression is mediated through the mitochondrial metabolic pathway.

IL-1RA promoted SOX2 expression via phosphorylation of EGFR and JNK downstream of mitochondrial metabolic pathway

To further investigate the signaling molecules involved in IL-1RA-associated OSCC malignancy, an antibody array was used to screen for the phosphorylation status of kinases affected by IL-1RA. Antibody array screening showed that the expression levels of phosphorylated EGFR (p-EGFR) and phosphorylated JNK (p-JNK) were increased in OECM-1 cells overexpressing IL-1RA

(See figure on next page.)

Fig. 3 Effect of IL-1RA expression on mitochondrial metabolism and reactive oxygen species (ROS) formation in OSCC cells. **A** Multiple status of mitochondrial metabolism was measured by oxygen consumption rate (OCR) using Agilent Seahorse XFe24 Analyzer via sequential delivery of the indicated mitochondrial modulators (oligomycin, FCCP, and a mixture of rotenone and antimycin A) to OECM-1 cells with overexpression of IL-1RA and control cells. **B–C** Basal OCR indicated by the slope (Δ RFU/ Δ min) was measured with CLARIOstar Plus multi-mode plate reader using a commercial oxygen consumption-labeling kit, for HSC-3 cells with knockdown of IL-1RA and control cells in (**B**), and OECM-1 cells with overexpression of IL-1RA and control cells in (**C**). **D–E** ROS formation was measured by flow cytometry after DCFDA labeling of OECM-1 cells with overexpression of IL-1RA and control cells in the presence or absence of rotenone in (**D**), and metformin or phenformin in (**E**). Data were presented as mean \pm SD from three independent experiments. *, $p < 0.05$; **, $p < 0.01$; ***, $p < 0.001$. RFU, relative fluorescence unit; shLuc, knockdown of firefly luciferase; shIL-1RA, knockdown of IL-1RA; EV, empty vector; IL-1RA-OE, overexpression of IL-1RA

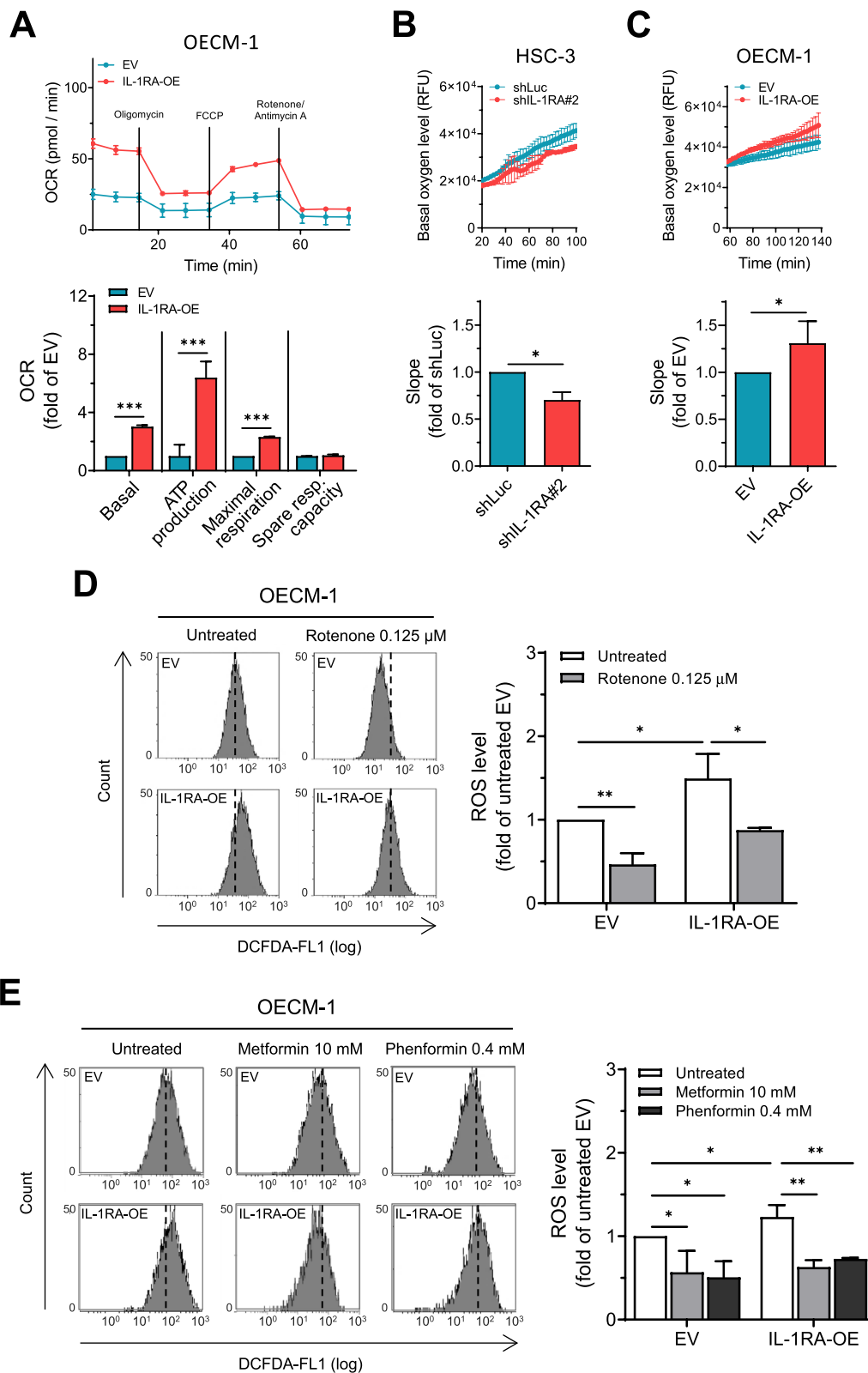


Fig. 3 (See legend on previous page.)

(Fig. 6A), which was confirmed by western blotting (Fig. 6B). The increase in p-EGFR and p-JNK induced by IL-1RA overexpression in OECM-1 cells was reduced in the presence of metformin, along with a reduction in EGFR and JNK expression (Fig. 6C). We also found that inhibition of EGFR by gefitinib (an EGFR inhibitor [38]) reduced the expression of p-JNK and SOX2 (Fig. 6D). In addition, a correlation between IL-1RA expression and the expression of p-EGFR (Fig. 6E) and p-JNK (Fig. 6F) was observed in oral tumor tissues from patients with OSCC. Taken together, these data suggest that IL-1RA-associated OSCC malignancy is regulated via EGFR-mediated JNK signaling and SOX2 expression, which lie downstream of the mitochondrial metabolic pathway.

IL-1RA-promoted in vivo tumor growth and p-EGFR/p-JNK/SOX2 expression were suppressed by metformin and cisplatin

The effect of IL-1RA on in vivo tumor growth was evaluated in mice via orthotopic xenografts of OECM-1-luc cells with IL-1RA overexpression or empty vector as a control (Additional file 1: Figure S6A), and the effect of treatment with metformin, cisplatin (also known as CDDP; a chemotherapeutic agent [39]), or a combination of both, was further evaluated (Additional file 1: Figure S6B). Tumor formation was measured weekly using an in vivo imaging system (IVIS). At the end of the experiment, a higher level of bioluminescence resulting from luciferase activity in the orthotopic xenograft area was observed in mice treated with IL-1RA-overexpressing OECM-1-luc cells (Fig. 7A). Furthermore, the mice treated with metformin, CDDP, or a combination of both showed reduced levels of bioluminescence (Fig. 7A), as well as reduced tumor weight (Fig. 7B) and tumor volume (Additional file 1: Figure S6C and D), in which the combined metformin and CDDP treatment exhibited the greatest effect on the inhibition of tumor formation. Immunohistochemical analysis for the expression of IL-1RA, Ki-67 (a cancer proliferation marker [40]), p-EGFR, p-JNK, and SOX2 revealed that IL-1RA expression remained high in the xenograft tumors collected from the mice groups with IL-1RA-overexpressing OECM-1-luc cells (Fig. 7C), whereas the elevated expression of IL-1RA-associated Ki-67, p-EGFR, p-JNK, and SOX2 was reduced in the groups treated with metformin, CDDP,

or a combination of both (Fig. 7D–G). These data suggested that IL-1RA promoted in vivo tumor growth with increased p-EGFR, p-JNK, and SOX2 expression, which was suppressed by treatment with metformin or CDDP. In addition, combined treatment with metformin and CDDP may have a greater biological effect than treatment with metformin or CDDP.

Discussion

IL-1RA, a critical regulator of the IL-1 signaling network, has emerged as a key player in cancer development [41, 42], yet its role in oral cancer malignancy remains to be elucidated. In this study, we highlighted the significance of IL-1RA as a clinical marker of OSCC and explored its biological mechanisms and therapeutic potential. Specifically, our data suggest that elevated IL-1RA levels are associated with adverse OSCC progression and poor patient outcomes. In addition, IL-1RA-promoted OSCC malignancy involved enhanced properties of cancer stemness via a mitochondrial metabolism-associated EGFR/JNK pathway, which may be suppressed by application of mitochondrial complex inhibitors both in vitro and in vivo (Fig. 8).

A novel IL-1RA/EGFR/JNK pathway in oral cancer

EGFR is a transmembrane protein that can transduce signals via translocation to intracellular organelles upon stimulation of various cancer cells, in addition to its canonical receptor tyrosine kinase activity [43–45]. For example, mitochondrial translocation of EGFR occurs in breast cancer cells in response to EGF stimulation, which subsequently induces the phosphorylation of cytochrome c oxidase subunit II (Cox II) in the mitochondria and enhances cancer cell survival [46, 47]. Mitochondrial translocation of EGFR following EGF stimulation was also observed in non-small cell lung cancer (NSCLC), where increased mitochondrial EGFR upregulates ATP production and enhances the metastatic ability of NSCLC cells [48]. Another study revealed that nuclear translocation of EGFR is regulated by AKT, which is associated with gefitinib resistance in breast cancer cells through enhanced gene expression of the breast cancer-resistant protein (*BCRP*; also known as ATP-binding cassette subfamily G member 2, *ABCG2*) [49]. Furthermore, attenuation of estrogen receptor β expression leads to

(See figure on next page.)

Fig. 4 Involvement of mitochondrial metabolism in IL-1RA-promoted malignant behaviors of OSCC cells. **A–B** OECM-1 cells with IL-1RA overexpression and control cells were assessed for tumorsphere formation in the presence or absence of rotenone or antimycin A in **(A)**, and metformin or phenformin in **(B)**. **C–D** OECM-1 cells with IL-1RA overexpression and control cells were assessed for transwell cell migration ability in the presence or absence of rotenone or antimycin A in **(C)**, and metformin or phenformin in **(D)**. **E** OECM-1 cells with IL-1RA overexpression and control cells were assessed for transwell cell invasion ability in the presence or absence of metformin or phenformin. Data were presented as mean \pm SD from three independent experiments. *, $p < 0.05$; **, $p < 0.01$; ***, $p < 0.001$. EV, empty vector; IL-1RA-OE, overexpression of IL-1RA

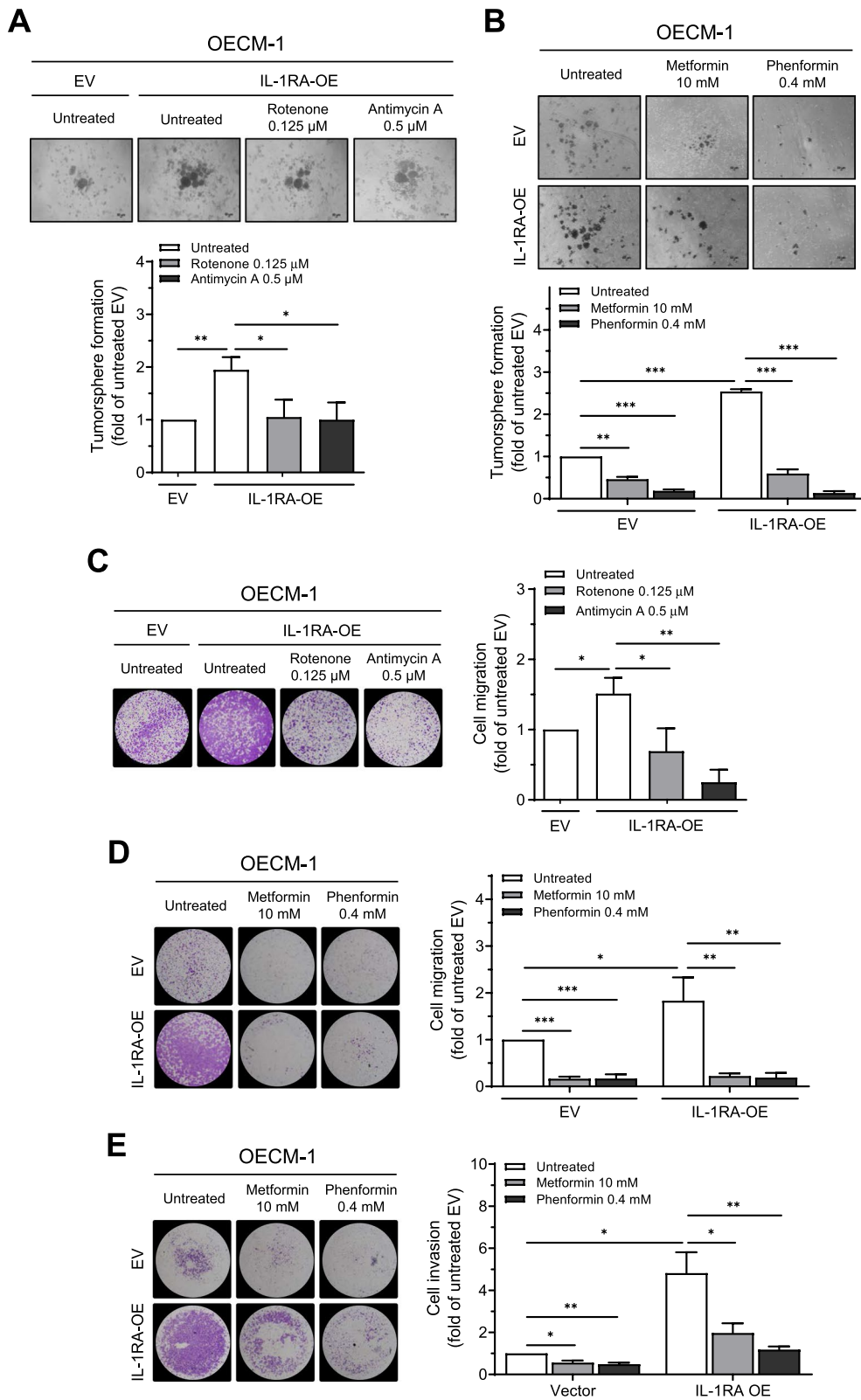


Fig. 4 (See legend on previous page.)

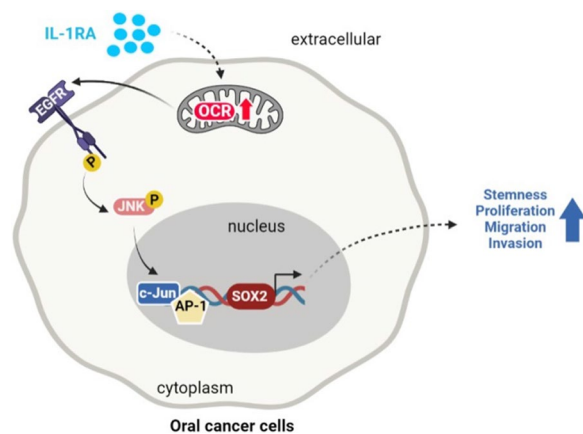


Fig. 5 Involvement of mitochondrial metabolism in the expression of IL-1RA-associated cancer stemness markers. **A** PCR array was applied to screen a set of cancer stem cell-related genes in HSC-3 cells with knockdown of IL-1RA, in which the expression of each gene was quantitated relative to that in control cells (dashed line). **B–C** Four candidates (SOX2, THY1, EGF, and KIT), as indicated by the solid rectangle in **(A)**, were further examined by Western blot for their protein expression in HSC-3 and Ca9-22 cells with knockdown of IL-1RA in **(B)**, and OECM-1 cells with overexpression of IL-1RA in **(C)**, along with the control cells. **D** Protein expression of SOX2 in OECM-1 cells with overexpression of IL-1RA and control cells was examined by Western blot in the presence or absence of rotenone or antimycin A. Data were presented as mean \pm SD from three independent experiments in **(B–D)**. *, $p < 0.05$; **, $p < 0.01$; ***, $p < 0.001$. Rot., rotenone; Ant. A, antimycin A; shLuc, knockdown of firefly luciferase; shIL-1RA, knockdown of IL-1RA; EV, empty vector; IL-1RA-OE, overexpression of IL-1RA

increased EGFR nuclear translocation, which is associated with poor patient outcomes in prostate cancer [50]. Our current study revealed for the first time that the activation of EGFR by IL-1RA induced the activation of the JNK pathway and was associated with enhanced malignant behavior of OSCC cells. Clinicopathological analysis supported these findings by revealing a positive correlation between the expression of IL-1RA and

phosphorylated EGFR and JNK in OSCC tumor tissues. This newly identified pathway involving IL-1RA/EGFR/JNK indicates that targeting the EGFR pathway may be a potential therapeutic strategy for IL-1RA-associated OSCC malignancy. Other than our study, it has also been reported that miR-100 promotes tumor metastasis in mouse breast cancer via the STAT5a/IL-1RA signaling pathway [51]. On the other hand, the anti-cancer activity of IL-1RA has been reported, with a previous study showing that IL-1RA suppresses esophageal cancer cell growth through inhibition of IL-1 α -VEGF signaling [52].

Along with our findings, KRAS has also been found to be associated with cell invasion, tumorigenesis, and lymph node metastasis in oral cancer [53]. Wang et al. demonstrated that KRAS is a novel prognostic marker in OSCC among Taiwanese people [54]. Oncogenic RAS targets metabolic reprogramming in various cancer types, including pancreatic cancer, lung cancer, colorectal cancer, and head and neck cancer [55]. Interestingly, combinational treatment of 5-fluorouracil and IL-1RA decreases the proliferation ability in colon cancer cells with KRAS mutation [56]. Although the cross-talk between IL-1RA and KRAS in oral cancer remains unclear, the underlying mechanism deserves further exploration.

OSCC cancer stemness is enhanced by IL-1RA

Cancer stemness, the enhanced ability for self-proliferation and cancer cell motility, has been shown to correlate with tumor recurrence and metastasis and is a critical area in oral cancer research [8, 57, 58]. Our current study showed that IL-1RA enhanced cancer stemness-associated properties of OSCC cells, such as self-proliferation, anchorage-independent growth, and cell migration/invasion abilities. In addition, IL-1RA promoted the expression of SOX2 in OSCC cells. As SOX2 is a pleiotropic transcription factor and an important hallmark of cancer stemness, with functional roles in regulating tumor growth and metastasis [59, 60], our current findings

(See figure on next page.)

Fig. 6 Involvement of mitochondrial metabolism in IL-1RA-associated EGFR/JNK activation and SOX2 expression. **A–B** Up-regulated phosphorylation of EGFR and JNK was shown by phospho-kinase proteome array screening for the phosphorylation status of a set of kinases, with duplicate detection for each kinase, in OECM-1 cells with overexpression of IL-1RA in **(A)**, which was further confirmed by Western blot in **(B)**. **C** Protein expression of phosphorylated EGFR and JNK, along with their unphosphorylated forms, in OECM-1 cells with overexpression of IL-1RA and control cells was examined by Western blot in the presence or absence of metformin. **D** Protein expression of phosphorylated EGFR and JNK, along with their unphosphorylated forms, and SOX2 in OECM-1 cells with overexpression of IL-1RA and control cells was examined by Western blot in the presence or absence of gefitinib. Data were presented as mean \pm SD from three independent experiments in **(B–D)**. *, $p < 0.05$; **, $p < 0.01$; ***, $p < 0.001$. **E–F** Correlation between IL-1RA expression and phosphorylation of EGFR **(E)** and JNK **(F)** in OSCC tumor tissues from patients was analyzed according to IHC scoring, and was evaluated by Pearson correlation (*r*). Met., metformin; Gef., gefitinib; p-EGFR, phosphorylated EGFR; p-JNK, phosphorylated JNK; EV, empty vector; IL-1RA-OE, overexpression of IL-1RA

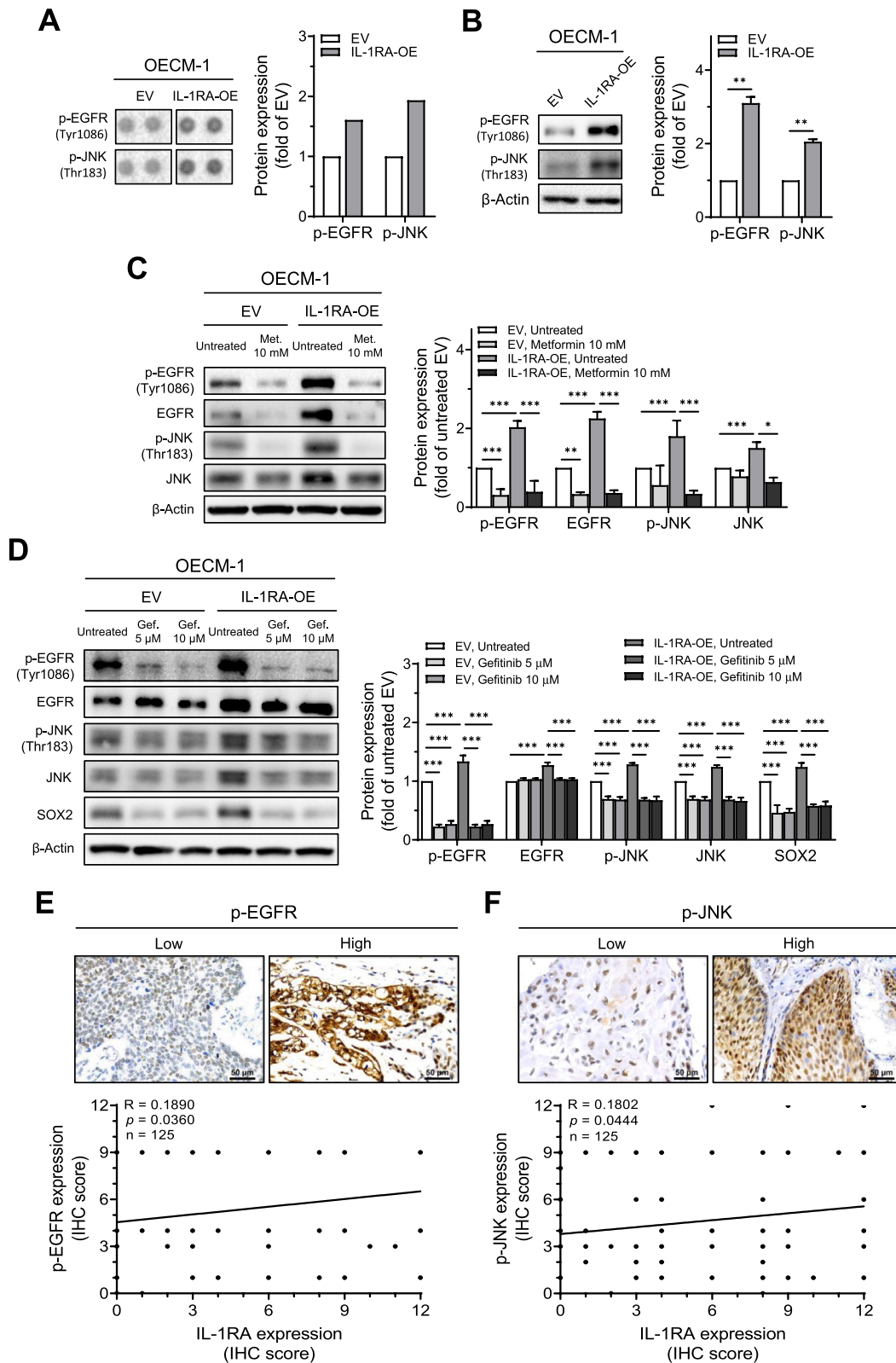


Fig. 6 (See legend on previous page.)

suggest that increased SOX2 expression may play a role in IL-1RA-promoted OSCC malignancy.

Inhibition of mitochondrial metabolism may abrogate IL-1RA-mediated malignant behaviors

Alteration of cellular energy and redox status via mitochondrial metabolism, a process known as mitochondrial metabolic reprogramming, has been shown to be associated with cancer progression [61, 62]. As a result, targeting mitochondria by inhibiting mitochondrial complexes presents a novel therapeutic strategy for cancer [63, 64]. Our in vitro data showed that IL-1RA overexpression increased the rate of mitochondrial oxidative metabolism and inhibition of mitochondrial electron transfer complexes, including the use of conventional compound inhibitors (e.g., metformin, phenformin, rotenone, or antimycin A [39, 65]) and novel peptide inhibitors (e.g., CT20 [66] or MITOx20 [67]), suppressed IL-1RA-promoted malignant behaviors of OSCC cells. In particular, the widely used diabetic medication metformin inhibits mitochondrial complex 1 to reduce tumorigenesis, with cancer risk reduction noted in epidemiological studies [68–70]. On the other hand, Cisplatin is a commonly used chemotherapeutic agent for treatment of oral cancer [71, 72]. The current study explored the potential of metformin as a therapeutic drug for IL-1RA-associated OSCC malignancy in an orthotopic xenograft mouse model, showing that IL-1RA-promoted tumor growth and activation of EGFR/JNK and SOX2 expression in tumor tissues was reduced by metformin or cisplatin treatment, and the inhibitory effect was further augmented by combination therapy. Together, these data not only suggest a crucial involvement of mitochondrial metabolism in IL-1RA-promoted OSCC growth with participation of the EGFR/JNK/SOX2 pathway but also provide pre-clinical evidence for drug repurposing of metformin as an adjunctive treatment in combination with existing cancer therapies to enhance the therapeutic response [73, 74]. Furthermore, our data may help identify those who would benefit most from such adjunctive treatments, suggesting risk stratification of patients with

high IL 1RA tumor tissue levels requiring radiotherapy to additional metformin treatment.

Limitations and future work

While this study has unveiled a novel mechanism underlying IL-1RA-promoted OSCC malignancy through mitochondrial metabolism-associated EGFR/JNK activation and SOX2 expression, there are some limitations inherent in our current data, as well as areas that warrant further investigation. A limitation of this study is that the clinical samples used in this study were all from the decoded biological database and therefore we were unable to study the effect of other underlying conditions on the expression of IL-1RA. Also, whether IL-1RA-activated EGFR transduces signals via its receptor tyrosine kinase activity or via translocation to intracellular organelles remains to be determined. The genetic control of SOX2 expression induced by IL-1RA in OSCC cells also requires further investigation, such as the potential for transcriptional regulation by c-Jun, which can bind to the promoter region of SOX2 [75, 76]. Furthermore, apart from the effect of metformin on in vivo tumor growth examined in this study, the therapeutic potential of metformin on metastasis in a pre-clinical in vivo model merits further investigation.

Conclusions

The current study demonstrates a critical role for IL-1RA in the pathogenesis of OSCC, and its elevated expression in OSCC tumor tissues may be considered an adverse clinical marker for cancer progression and treatment response. In addition, the newly identified biological mechanisms linking IL-1RA and OSCC malignancy suggest that mitochondrial metabolism plays a crucial role in regulating the malignant behavior of OSCC cells. In particular, the administration of metformin, which has been proposed as a repurposed drug for cancer treatment [68, 69, 73, 74], alleviates IL-1RA-promoted OSCC malignancy through EGFR/JNK signaling and SOX2 expression. These findings not only reveal the impact of IL-1RA and its associated mechanisms on OSCC malignancy but

(See figure on next page.)

Fig. 7 Effect of IL-1RA expression on in vivo tumor growth of OSCC in xenograft mice and the therapeutic potential of metformin. **A** Orthotopic xenograft of OECM-1 cells with overexpression of IL-1RA or control cells in mice was measured weekly by in vivo imaging system (IVIS) for the groups treated with or without metformin and/or CDDP. The data shown in **(A)** were the measurements at endpoint of the experiment before sacrifice of the mice. **B** After sacrifice of the mice at endpoint of the experiment, the xenograft tumors were collected and tumor weight was measured. **C–G** After sacrifice of the mice at endpoint of the experiment, the xenograft tumors were collected and analyzed for protein expression of IL-1RA **(C)**, Ki67 **(D)**, phosphorylated EGFR **(E)**, phosphorylated JNK **(F)**, and SOX2 **(G)**. Data were presented as mean \pm SD from five mice in each group. *, $p < 0.05$; **, $p < 0.01$; ***, $p < 0.001$. CDDP, cisplatin; p-EGFR, phosphorylated EGFR; p-JNK, phosphorylated JNK; EV, empty vector; IL-1RA-OE, overexpression of IL-1RA

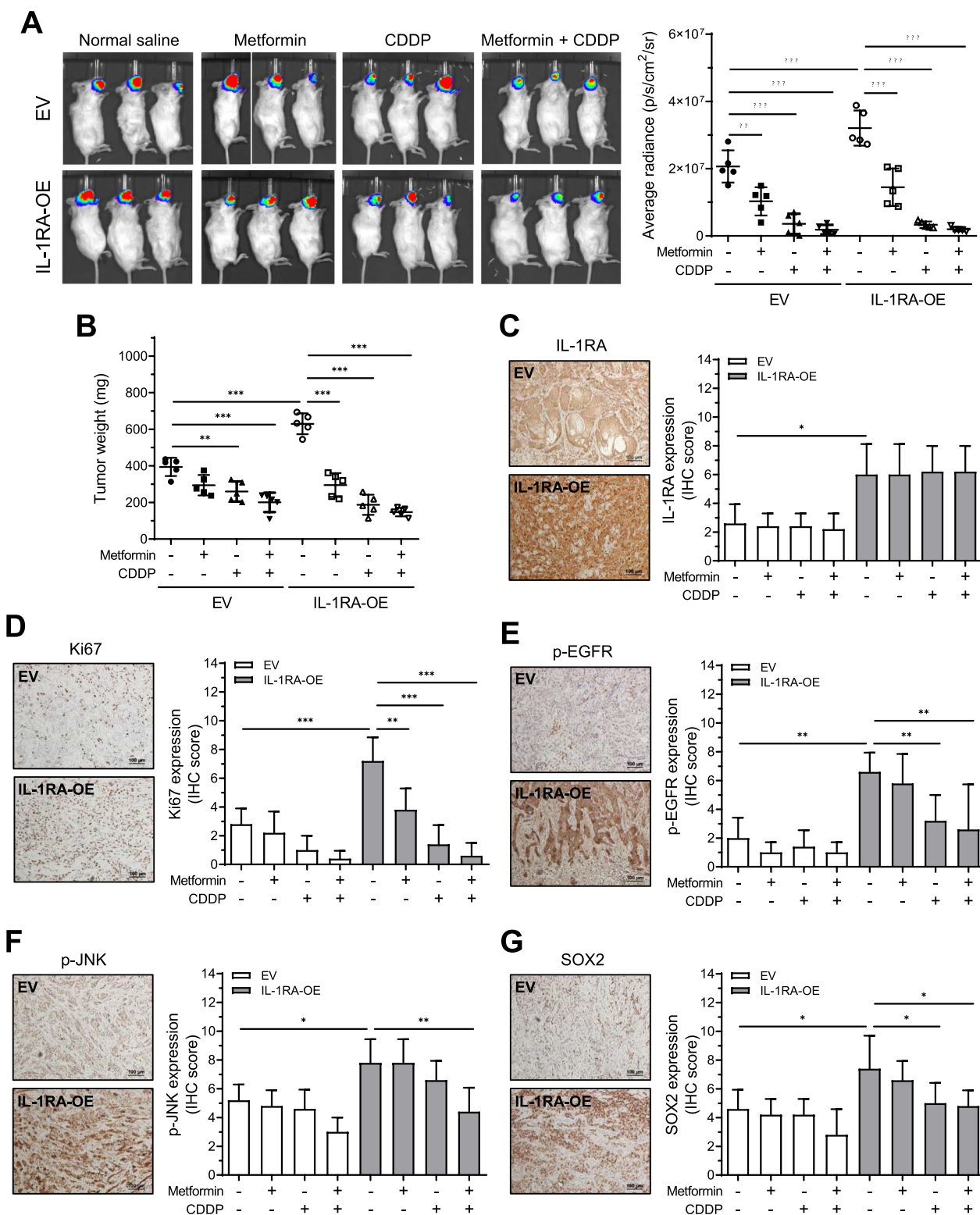


Fig. 7 (See legend on previous page.)

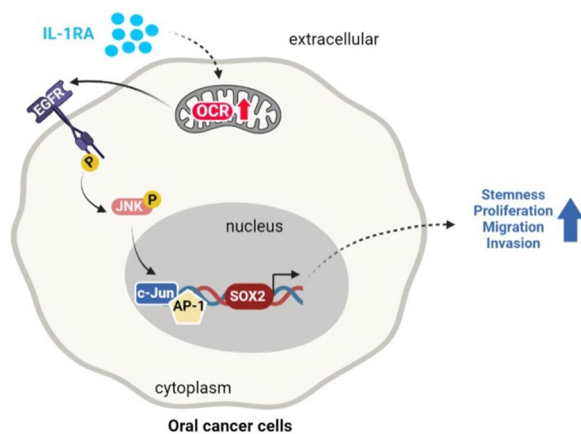


Fig. 8 Schematic summary for the current study. The results of the current study suggest that mitochondrial metabolism may be crucial in mediating the IL-1RA-promoted malignant behaviors of OSCC cells, such as cancer stemness-associated tumor growth and migration/invasion abilities, through a pathway involving EGFR/JNK activation and SOX2 expression

also provide insights for further development of targeted therapies, such as the potential for targeted delivery of metformin to mitochondria [77] or cancer cell surfaces [78], as a treatment strategy for OSCC.

Abbreviations

ANOVA	One-way analysis of variance
ECAR	Extracellular acidification rate
EGF	Epidermal growth factor
EGFR	Epidermal growth factor receptor
EV	Empty vector
FBS	Fetal bovine serum
FGF-basic	Fibroblast growth factor-basic
FCCP	Carbonyl cyanide 4-(trifluoromethoxy)phenylhydrazone
GAPDH	Glyceraldehyde-3-phosphate dehydrogenase
IHC	Immunohistochemistry
IL-1	Interleukin-1
IL-1RA	Interleukin-1 receptor antagonist
IL-1RA-OE	Overexpression of IL-1RA
IR	Ionizing radiation
IVIS	In vivo imaging system
JNK	C-Jun N-terminal kinase
OCR	Oxygen consumption rate
OSCC	Oral squamous cell carcinoma
PCR	Polymerase chain reaction
RFU	Relative fluorescence unit
ROS	Reactive oxygen species
SDS-PAGE	Sodium dodecyl sulfate–polyacrylamide gel electrophoresis
shIL-1RA	Knockdown of IL-1RA
shLuc	Knockdown of firefly luciferase
SOX2	SRY-box transcription factor 2

Supplementary Information

The online version contains supplementary material available at <https://doi.org/10.1186/s12967-023-04343-9>.

Additional file 1: Figure S1. A Endogenous protein expression of IL-1RA was examined by Western blot in four human OSCC cell lines, including HSC-3, SAS, Ca9-22, and OECM-1 cells, along with human dysplastic

oral keratinocyte (DOK) cells for comparison. Data were presented as mean \pm SD from three independent experiments, and the number indicates fold of protein expression in each cell line relative to DOK cells. **B** Representative results by Western blot showed the knockdown efficiency from four clones of shRNA targeting different consensus regions of human *IL1RN* (Accession: NM_000577). The number indicates fold of protein expression in HSC-3 cells carrying individual shRNA clone relative to the control cells. **C** Representative results by Western blot showed the protein expression of knockdown of IL-1RA in HSC-3 or Ca9-22 cells using shRNA clones #1 and #2 that had a better knockdown efficiency compared to shRNA clones #3 and #4 in **(B)**, and the protein expression of overexpression of IL-1RA in OECM-1 cells carrying a vector that expresses full-length human *IL1RN* (Accession: NM_173841.2). GAPDH, glyceraldehyde-3-phosphate dehydrogenase; shLuc, knockdown of firefly luciferase; shIL-1RA, knockdown of IL-1RA; EV, empty vector; IL-1RA-OE, overexpression of IL-1RA. **Figure S2. A-B** Cell cycle distribution was analyzed by flow cytometry in HSC-3 cells with knockdown of IL-1RA in **(A)**, and OECM-1 cells with overexpression of IL-1RA in **(B)**, along with the control cells. **C-D** Protein expression of p21 was examined by Western blot in HSC-3 cells with knockdown of IL-1RA in **(C)**, and OECM-1 cells with overexpression of IL-1RA in **(D)**, along with the control cells. Data were presented as mean \pm SD from three independent experiments. *, $p < 0.05$; **, $p < 0.01$. shLuc, knockdown of firefly luciferase; shIL-1RA, knockdown of IL-1RA; EV, empty vector; IL-1RA-OE, overexpression of IL-1RA. **Figure S3. A-B** Basal extracellular acidification rate (ECAR) indicated by the slope (Δ RFU/ Δ min) was measured in CLARIOstar Plus multi-mode plate reader using a commercial glycolytic flux-labeling kit for HSC-3 cells with knockdown of IL-1RA in **(A)**, and OECM-1 cells with overexpression of IL-1RA in **(B)**, along with the control cells. Data were presented as mean \pm SD from three independent experiments. *, $p < 0.05$; **, $p < 0.01$. shLuc, knockdown of firefly luciferase; shIL-1RA, knockdown of IL-1RA; EV, empty vector; IL-1RA-OE, overexpression of IL-1RA. **Figure S4. A** Overexpression of IL-1RA in OECM-1 cells and the control cells were assessed for transwell cell migration ability in the presence or absence of CT20 or MITOx20. **B-C** Overexpression of IL-1RA in OECM-1 cells and the control cells were assessed for cell viability by XTT assay in the presence or absence of rotenone or antimycin A in **(B)**, metformin or phenformin in **(C)**, and CT20 or MITOx20 in **(D)**. Data were presented as mean \pm SD from three independent experiments. **, $p < 0.01$. EV, empty vector; IL-1RA-OE, overexpression of IL-1RA. **Figure S5.** List of the genes screened by PCR array as shown in Fig. 5. **Figure S6. A** Representative results by Western blot showed the protein expression of overexpression of IL-1RA in OECM-1-luc cells carrying a vector that expresses full-length human *IL1RN* (Accession: NM_173841.2). **B** Schematic summary of the animal study. **C** Photograph of xenograft tumors collected from each group at endpoint of the experiment. **D** Xenograft tumors collected at endpoint of the experiment were measured for tumor volumes. CDDP, cisplatin; EV, empty vector; IL-1RA-OE, overexpression of IL-1RA.

Acknowledgements

Not applicable.

Author contributions

SSFY, YMW, LPC, ACH, HDHN, YKC, SCSH, SL, YYW conceived and designed the study. SSFY, YMW, LPC, ACH and YYW performed experiments. SSFY, YMW, HDHN, YKC and YYW analyzed and interpreted the data. SSFY and YYW prepared the manuscript. YMW, LPC, ACH, HDHN, YKC, SCSH and SL revised the manuscript critically. All authors have reviewed and approved the final manuscript.

Funding

This work was supported by grants from the Ministry of Science and Technology (MOST 111-2314-B-037-011-, MOST 111-2314-B-037-020-, MOST 111-2314-B-037-046-) and the Center for Intelligent Drug Systems and Smart Bio-devices (IDS²B) from the Featured Areas Research Center Program within the framework of the Higher Education Sprout Project by the Ministry of Education, Taiwan. This work was also supported by grants from Kaohsiung Medical University Hospital (KMUH110-0R43, KMUH110-0M65, KMUH111-1M56, KMUH111-1R37, KMUH-DK(A)112001) and Kaohsiung Medical University (KMU-DK(A)112006, NYCU-KMU-112-1005), Taiwan.

Availability of data and materials

The datasets used and/or analyzed during the current study are available from the corresponding author upon reasonable request.

Declarations**Ethics approval and consent to participate**

This study was approved by the Institutional Review Board of Kaohsiung Medical University Hospital (approval no. KMH-IRB-20130300 and KMH-IRB-F(I)-20220016). Patient informed consent was waived by the Institutional Review Board due to the retrospective nature of the study. All animal experiments were approved by the Institutional Animal Care and Utilization Committee of Kaohsiung Medical University, Kaohsiung, Taiwan (approval no. 108127).

Consent for publication

Not applicable.

Competing interests

The authors declare that they have no competing interests.

Author details

¹Graduate Institute of Medicine, College of Medicine, Kaohsiung Medical University, Kaohsiung 807, Taiwan. ²Department of Medical Research, Kaohsiung Medical University Hospital, Kaohsiung 807, Taiwan. ³Department of Obstetrics and Gynecology, Kaohsiung Medical University Hospital, Kaohsiung 807, Taiwan. ⁴Translational Research Center, Kaohsiung Medical University Hospital, Kaohsiung 807, Taiwan. ⁵Drug Development and Value Creation Research Center, Kaohsiung Medical University, Kaohsiung 807, Taiwan. ⁶Department of Biological Science and Technology, Institute of Molecular Medicine and Bioengineering, Center for Intelligent Drug Systems and Smart Bio-devices (IDS2B), National Yang Ming Chiao Tung University, 75 Bo-Ai Street, Hsinchu 300, Taiwan. ⁷School of Dentistry, College of Dental Medicine, Kaohsiung Medical University, No.100, Shih-Chuan 1st Road, Sanmin Dist., Kaohsiung 80708, Taiwan. ⁸Cohort Research Center, Kaohsiung Medical University, Kaohsiung 807, Taiwan. ⁹Faculty of Medicine, College of Medicine, Kaohsiung Medical University, Kaohsiung 807, Taiwan. ¹⁰Department of Otorhinolaryngology-Head and Neck Surgery, Kaohsiung Municipal Ta-Tung Hospital and Kaohsiung Medical University Hospital, Kaohsiung 807, Taiwan. ¹¹Division of Oral Pathology & Maxillofacial Radiology, Kaohsiung Medical University Hospital, Kaohsiung 807, Taiwan. ¹²Department of Dermatology, College of Medicine, Kaohsiung Medical University, Kaohsiung 807, Taiwan. ¹³Department of Dermatology, Kaohsiung Medical University Hospital, Kaohsiung 807, Taiwan. ¹⁴Canniesburn Regional Plastic Surgery and Burns Unit, Glasgow G4 0SF, UK. ¹⁵College of Medical, Veterinary and Life Sciences, University of Glasgow, Glasgow G12 8QQ, UK.

Received: 30 May 2023 Accepted: 10 July 2023

Published online: 17 July 2023

References

- Du M, Nair R, Jamieson L, Liu Z, Bi P. Incidence trends of lip, oral cavity, and pharyngeal cancers: global burden of disease 1990–2017. *J Dent Res*. 2020;99(2):143–51.
- Rivera C. Essentials of oral cancer. *Int J Clin Exp Pathol*. 2015;8(9):11884–94.
- Sung H, Ferlay J, Siegel RL, Laversanne M, Soerjomataram I, Jemal A, Bray F. Global cancer statistics 2020: GLOBOCAN estimates of incidence and mortality worldwide for 36 cancers in 185 countries. *CA Cancer J Clin*. 2021;71(3):209–49.
- Coletta RD, Yeudall WA, Salo T. Grand challenges in oral cancers. *Front Oral Health*. 2020;1:3.
- Cheng Y, Li S, Gao L, Zhi K, Ren W. The molecular basis and therapeutic aspects of cisplatin resistance in oral squamous cell carcinoma. *Front Oncol*. 2021;11:761379.
- Vig N, Mackenzie IC, Biddle A. Phenotypic plasticity and epithelial-to-mesenchymal transition in the behaviour and therapeutic response of oral squamous cell carcinoma. *J Oral Pathol Med*. 2015;44(9):649–55.
- Lee SY, Jeong EK, Ju MK, Jeon HM, Kim MY, Kim CH, Park HG, Han SI, Kang HS. Induction of metastasis, cancer stem cell phenotype, and oncogenic metabolism in cancer cells by ionizing radiation. *Mol Cancer*. 2017;16(1):10.
- Liu Y, Yang M, Luo J, Zhou H. Radiotherapy targeting cancer stem cells “awakens” them to induce tumour relapse and metastasis in oral cancer. *Int J Oral Sci*. 2020;12(1):19.
- Moindjie H, Rodrigues-Ferreira S, Nahmias C. Mitochondrial metabolism in carcinogenesis and cancer therapy. *Cancers*. 2021;13(13):3311.
- Sotgia F, Fiorillo M, Lisanti MP. Hallmarks of the cancer cell of origin: comparisons with “energetic” cancer stem cells (e-CSCs). *Aging*. 2019;11(3):1065–8.
- Yazdi AS, Ghoreschi K. The interleukin-1 family. *Regul Cytokine Gene Expr Immun Dis*. 2021;941:21–9.
- Akash MS, Rehman K, Chen S. IL-1Ra and its delivery strategies: inserting the association in perspective. *Pharmaceut Res*. 2013;30:2951–66.
- Dinarello CA. Interleukin-1, interleukin-1 receptors and interleukin-1 receptor antagonist. *Int Rev Immunol*. 1998;16(5–6):457–99.
- Eisenberg SP, Evans RJ, Arend WP, Verderber E, Brewer MT, Hannum CH, Thompson RC. Primary structure and functional expression from complementary DNA of a human interleukin-1 receptor antagonist. *Nature*. 1990;343(6256):341–6.
- Iwagaki H, Hizuta A, Tanaka N. Interleukin-1 receptor antagonists and other markers in colorectal cancer patients. *Scand J Gastroenterol*. 1997;32(6):577–81.
- Kurzrock R. Cytokine deregulation in cancer. *Biomed Pharmacother*. 2001;55(9–10):543–7.
- Parekh DJ, Ankerst DP, Baillargeon J, Higgins B, Platz EA, Troyer D, Hernandez J, Leach RJ, Lokshin A, Thompson IM. Assessment of 54 biomarkers for biopsy-detectable prostate cancer. *Cancer Epidemiol Biomarkers Prev*. 2007;16(10):1966–72.
- Shiiba M, Saito K, Yamagami H, Nakashima D, Higo M, Kasamatsu A, Sakamoto Y, Ogawara K, Uzawa K, Takiguchi Y, Tanzawa H. Interleukin-1 receptor antagonist (IL1RN) is associated with suppression of early carcinogenic events in human oral malignancies. *Int J Oncol*. 2015;46(5):1978–84.
- Fujiwaki R, Iida K, Nakayama K, Kanasaki H, Hata K, Katabuchi H, Okamura H, Miyazaki K. Clinical significance of interleukin-1 receptor antagonist in patients with cervical carcinoma. *Gynecol Oncol*. 2003;89(1):77–83.
- Iizuka N, Hazama S, Hirose K, Abe T, Tokuda N, Fukumoto T, Tangoku A, Oka M. Interleukin-1 receptor antagonist mRNA expression and the progression of gastric carcinoma. *Cancer Lett*. 1999;142(2):179–84.
- Niklander SE, Murdoch C, Hunter KD. IL-1/IL-1R signaling in head and neck cancer. *Front oral health*. 2021;2:722676.
- Yang YF, Wang YY, Hsiao M, Lo S, Chang YC, Jan YH, Lai TC, Lee YC, Hsieh YC, Yuan SF. IMPAD1 functions as mitochondrial electron transport inhibitor that prevents ROS production and promotes lung cancer metastasis through the AMPK-Notch1-HEY1 pathway. *Cancer Lett*. 2020;485:27–37.
- Zhang J, Zhang Q. Using Seahorse machine to measure OCR and ECAR in cancer cells. *Methods Mol Biol*. 1928;353–363:2019.
- Wang YY, Chen YK, Lo S, Chi TC, Chen YH, Hu SC, Chen YW, Jiang SS, Tsai FY, Liu W, Li RN, Hsieh YC, Huang CJ, Yuan SF. MRE11 promotes oral cancer progression through RUNX2/CXCR4/AKT/FOXO2 signaling in a nuclease-independent manner. *Oncogene*. 2021;40(20):3510–32.
- Wang YY, Chen HD, Lo S, Chen YK, Huang YC, Hu SC, Hsieh YC, Hung AC, Hou MF, Yuan SF. Visfatin enhances breast cancer progression through CXCL1 induction in tumor-associated macrophages. *Cancers*. 2020;12(12):3526.
- Wang YY, Hung AC, Wu YC, Lo S, Chen HD, Chen YK, Hsieh YC, Hu SC, Hou MF, Yuan SF. ADSCs stimulated by resistin promote breast cancer cell malignancy via CXCL5 in a breast cancer coculture model. *Sci Rep*. 2022;12(1):15437.
- Yuan SF, Hung AC, Hsu CW, Lan TH, Su CW, Chi TC, Chang YC, Chen YK, Wang YY. CD44 mediates oral squamous cell carcinoma-promoting activity of MRE11 via AKT signaling. *J Pers Med*. 2022;12(5):841.
- Reya T, Morrison SJ, Clarke MF, Weissman IL. Stem cells, cancer, and cancer stem cells. *Nature*. 2001;414(6859):105–11.

29. Bahmad HF, Cheaito K, Chalhoub RM, Hadadeh O, Monzer A, Ballout F, El-Hajj A, Mukherji D, Liu YN, Daoud G, Abou-Kheir W. Sphere-formation assay: three-dimensional in vitro culturing of prostate cancer stem/progenitor sphere-forming cells. *Front Oncol.* 2018;8:347.
30. Agrez MV, Kovach JS, Lieber MM. Cell aggregates in the soft agar "human tumour stem-cell assay." *Br J Cancer.* 1982;46(6):880–7.
31. Brix N, Samaga D, Belka C, Zitzelsberger H, Lauber K. Analysis of clonogenic growth in vitro. *Nat Protoc.* 2021;16(11):4963–91.
32. Weiswald LB, Bellet D, Dangles-Marie V. Spherical cancer models in tumor biology. *Neoplasia.* 2015;17(1):1–15.
33. Diehn M, Cho RW, Lobo NA, Kalisky T, Dorie MJ, Kulp AN, Qian D, Lam JS, Ailles LE, Wong M, Joshua B, Kaplan MJ, Wapnir I, Dirbas FM, Somlo G, Garberoglio C, Paz B, Shen J, Lau SK, Quake SR, Brown JM, Weissman IL, Clarke MF. Association of reactive oxygen species levels and radioresistance in cancer stem cells. *Nature.* 2009;458(7239):780–3.
34. Marchetti P, Fovez Q, Germain N, Khamari R, Kluz J. Mitochondrial spare respiratory capacity: mechanisms, regulation, and significance in non-transformed and cancer cells. *FASEB J.* 2020;34(10):13106–24.
35. Schmidt CA, Fisher-Wellman KH, Neuffer PD. From OCR and ECAR to energy: perspectives on the design and interpretation of bioenergetics studies. *J Biol Chem.* 2021;297(4):101140.
36. Koopman WJ, Nijtmans LG, Dieteren CE, Roestenberg P, Valsecchi F, Smeitink JA, Willems PH. Mammalian mitochondrial complex I: biogenesis, regulation, and reactive oxygen species generation. *Antioxid Redox Signal.* 2010;12(12):1431–70.
37. Murai M, Miyoshi H. Current topics on inhibitors of respiratory complex I. *Biochim Biophys Acta.* 2016;1857(7):884–91.
38. Ono M, Kuwano M. Molecular mechanisms of epidermal growth factor receptor (EGFR) activation and response to gefitinib and other EGFR-targeting drugs. *Clin Cancer Res.* 2006;12(24):7242–51.
39. Forgie BN, Prakash R, Telleria CM. Revisiting the anti-cancer toxicity of clinically approved platinum derivatives. *Int J Mol Sci.* 2022;23(23):15410.
40. Andres-Sanchez N, Fisher D, Krasinska L. Physiological functions and roles in cancer of the proliferation marker Ki-67. *J Cell Sci.* 2022. <https://doi.org/10.1242/jcs.258932>.
41. Boersma B, Jiskoot W, Lowe P, Bourquin C. The interleukin-1 cytokine family members: role in cancer pathogenesis and potential therapeutic applications in cancer immunotherapy. *Cytokine Growth Factor Rev.* 2021;62:1–14.
42. Mantovani A, Barajon I, Garlanda C. IL-1 and IL-1 regulatory pathways in cancer progression and therapy. *Immunol Rev.* 2018;281(1):57–61.
43. Sigismund S, Avanzato D, Lanzetti L. Emerging functions of the EGFR in cancer. *Mol Oncol.* 2018;12(1):3–20.
44. Tomas A, Futter CE, Eden ER. EGF receptor trafficking: consequences for signaling and cancer. *Trends Cell Biol.* 2014;24(1):26–34.
45. Wang YN, Hung MC. Nuclear functions and subcellular trafficking mechanisms of the epidermal growth factor receptor family. *Cell Biosci.* 2012;2(1):13.
46. Boerner JL, Demory ML, Silva C, Parsons SJ. Phosphorylation of Y845 on the epidermal growth factor receptor mediates binding to the mitochondrial protein cytochrome c oxidase subunit II. *Mol Cell Biol.* 2004;24(16):7059–71.
47. Demory ML, Boerner JL, Davidson R, Faust W, Miyake T, Lee I, Huttemann M, Douglas R, Haddad G, Parsons SJ. Epidermal growth factor receptor translocation to the mitochondria: regulation and effect. *J Biol Chem.* 2009;284(52):36592–604.
48. Che TF, Lin CW, Wu YY, Chen YJ, Han CL, Chang YL, Wu CT, Hsiao TH, Hong TM, Yang PC. Mitochondrial translocation of EGFR regulates mitochondria dynamics and promotes metastasis in NSCLC. *Oncotarget.* 2015;6(35):37349–66.
49. Huang WC, Chen YJ, Li LY, Wei YL, Hsu SC, Tsai SL, Chiu PC, Huang WP, Wang YN, Chen CH, Chang WC, Chang WC, Chen AJ, Tsai CH, Hung MC. Nuclear translocation of epidermal growth factor receptor by Akt-dependent phosphorylation enhances breast cancer-resistant protein expression in gefitinib-resistant cells. *J Biol Chem.* 2011;286(23):20558–68.
50. Wu WF, Wang L, Spetsieris N, Boukvala M, Efstathiou E, Brossner C, Warner M, Gustafsson JA. Estrogen receptor β and treatment with a phytoestrogen are associated with inhibition of nuclear translocation of EGFR in the prostate. *Proc Natl Acad Sci U S A.* 2021;118(13):e2011269118.
51. Wang W, Liu Y, Guo J, He H, Mi X, Chen C, Xie J, Wang S, Wu P, Cao F, Bai L. miR-100 maintains phenotype of tumor-associated macrophages by targeting mTOR to promote tumor metastasis via Stat5a/IL-1ra pathway in mouse breast cancer. *Oncogenesis.* 2018;7(12):97.
52. Chen S, Shen Z, Liu Z, Gao L, Han Z, Yu S, Kang M. IL-1RA suppresses esophageal cancer cell growth by blocking IL-1 α . *J Clin Lab Anal.* 2019;33(6):e22903.
53. El-hanbuli HM, Abou Sarie MA. KRAS protein expression in oral squamous cell carcinoma: a potential marker for progression and prognosis. *Iran J Pathol.* 2022;10:464–74.
54. Wang HC, Chiang CJ, Liu TC, Wu CC, Chen YT, Chang JG, Shieh GS. Immunohistochemical expression of five protein combinations revealed as prognostic markers in Asian oral cancer. *Front Genet.* 2021;12:643461.
55. Mukhopadhyay S, Vander Heiden MG, McCormick F. The metabolic landscape of RAS-driven cancers from biology to therapy. *Nat Cancer.* 2021;2(3):271–83.
56. Yan Y, Lin HW, Zhuang ZN, Li M, Guo S. Interleukin-1 receptor antagonist enhances chemosensitivity to fluorouracil in treatment of Kras mutant colon cancer. *World J Gastrointest Oncol.* 2020;2(8):877.
57. Sinha N, Mukhopadhyay S, Das DN, Panda PK, Bhutia SK. Relevance of cancer initiating/stem cells in carcinogenesis and therapy resistance in oral cancer. *Oral Oncol.* 2013;49(9):854–62.
58. Wolmarans E, Boy SC, Nel S, Mercier AE, Pepper MS. Cancer stem cells in head and neck carcinomas: identification and possible therapeutic implications. *Adv Exp Med Biol.* 2018;1083:89–102.
59. Mirzaei S, Paskeh MDA, Entezari M, Mirmazloomi SR, Hassanpoor A, Aboutalebi M, Rezaei S, Hejazi ES, Kakavand A, Heidari H, Salimimoghadam S, Taheriazam A, Hashemi M, Samarghandian S. SOX2 function in cancers: association with growth, invasion, stemness and therapy response. *Biomed Pharmacother.* 2022;156:113860.
60. Porter L, McCaughan F. SOX2 and squamous cancers. *Semin Cancer Biol.* 2020;67(Pt 1):154–67.
61. Choudhury FK. Mitochondrial redox metabolism: the epicenter of metabolism during cancer progression. *Antioxidants.* 2021;10(11):1838.
62. Zheng J. Energy metabolism of cancer: glycolysis versus oxidative phosphorylation. *Oncol Lett.* 2012;4(6):1151–7.
63. Bian C, Zheng Z, Su J, Wang H, Chang S, Xin Y, Jiang X. Targeting mitochondrial metabolism to reverse radioresistance: an alternative to glucose metabolism. *Antioxidants.* 2022;11(11):2202.
64. Yan L, Tan Y, Chen G, Fan J, Zhang J. Harnessing metabolic reprogramming to improve cancer immunotherapy. *Int J Mol Sci.* 2021;22(19):10268.
65. Fisher N, Meunier B, Biagini GA. The cytochrome bc₁ complex as an antipathogenic target. *FEBS Lett.* 2020;594(18):2935–52.
66. Lee MW, Bassiouni R, Sparrow NA, Iketani A, Boohaker RJ, Moskowitz C, Vishnubhotla P, Khaled AS, Oyer J, Copik A, Fernandez-Valle C, Perez JM, Khaled AR. The CT20 peptide causes detachment and death of metastatic breast cancer cells by promoting mitochondrial aggregation and cytoskeletal disruption. *Cell Death Dis.* 2014;5(5):e1249.
67. Giddings EL, Champagne DP, Wu MH, Laffin JM, Thornton TM, Valencapereira F, Culp-Hill R, Fortner KA, Romero N, East J, Cao P, Arias-Pulido H, Sidhu KS, Silverstrim B, Kam Y, Kelley S, Pereira M, Bates SE, Bunn JY, Fiering SN, Matthews DE, Robey RW, Stich D, D'Alessandro A, Rincon M. Mitochondrial ATP fuels ABC transporter-mediated drug efflux in cancer chemoresistance. *Nat Commun.* 2021;12(1):2804.
68. Chae YK, Arya A, Malecek MK, Shin DS, Carneiro B, Chandra S, Kaplan J, Kalyan A, Altman JK, Platanius L, Giles F. Repurposing metformin for cancer treatment: current clinical studies. *Oncotarget.* 2016;7(26):40767–80.
69. Kourelis TV, Siegel RD. Metformin and cancer: new applications for an old drug. *Med Oncol.* 2012;29(2):1314–27.
70. Wheaton WW, Weinberg SE, Hamanaka RB, Soberanes S, Sullivan LB, Anso E, Glasauer A, Dufour E, Mutlu GM, Budigner GS, Chandel NS. Metformin inhibits mitochondrial complex I of cancer cells to reduce tumorigenesis. *Elife.* 2014;3:e02242.
71. Johnson DE, Burtneis B, Leemans CR, Lui VW, Bauman JE, Grandis JR. Head and neck squamous cell carcinoma. *Nat Rev Dis Primers.* 2020;6(1):92.
72. Machiels JP, Leemans CR, Golusinski W, Grau C, Licitra L, Gregoire V. Squamous cell carcinoma of the oral cavity, larynx, oropharynx and hypopharynx: EHNS-ESMO-ESTRO clinical practice guidelines for diagnosis, treatment and follow-up. *Ann Oncol.* 2020;31(11):1462–75.
73. Deng J, Peng M, Wang Z, Zhou S, Xiao D, Deng J, Yang X, Peng J, Yang X. Novel application of metformin combined with targeted drugs on anticancer treatment. *Cancer Sci.* 2019;110(1):23–30.
74. Zhang HH, Guo XL. Combinational strategies of metformin and chemotherapy in cancers. *Cancer Chemother Pharmacol.* 2016;78(1):13–26.
75. Chang CC, Hsu WH, Wang CC, Chou CH, Kuo MY, Lin BR, Chen ST, Tai SK, Kuo ML, Yang MH. Connective tissue growth factor activates pluripotency

genes and mesenchymal-epithelial transition in head and neck cancer cells. *Cancer Res.* 2013;73(13):4147–57.

76. Chen H, Jin K, Song J, Zuo Q, Yang H, Zhang Y, Li B. Functional characterization of the *Sox2*, *c-Myc*, and *Oct4* promoters. *J Cell Biochem.* 2019;120(1):332–42.
77. Cheng G, Zielonka J, Ouari O, Lopez M, McAllister D, Boyle K, Barrios CS, Weber JJ, Johnson BD, Hardy M, Dwinell MB, Kalyanaraman B. Mitochondria-targeted analogues of metformin exhibit enhanced antiproliferative and radiosensitizing effects in pancreatic cancer cells. *Cancer Res.* 2016;76(13):3904–15.
78. Zhang F, Liu W, Long Y, Peng H. Targeted delivery of metformin against lung cancer cells via hyaluronan-modified mesoporous silica nanoparticles. *Appl Biochem Biotechnol.* 2023. <https://doi.org/10.1007/s12010-022-04289-6>.

Publisher's Note

Springer Nature remains neutral with regard to jurisdictional claims in published maps and institutional affiliations.

Ready to submit your research? Choose BMC and benefit from:

- fast, convenient online submission
- thorough peer review by experienced researchers in your field
- rapid publication on acceptance
- support for research data, including large and complex data types
- gold Open Access which fosters wider collaboration and increased citations
- maximum visibility for your research: over 100M website views per year

At BMC, research is always in progress.

Learn more biomedcentral.com/submissions

